Journal of Alloys and Compounds 504 (2010) L21–L24

Contents lists available at ScienceDirect

Journal of Alloys and Compounds

journal homepage: www.elsevier.com/locate/jallcom

Letter

Anode-supported $LaGaO_3$-based electrolyte SOFCs with Y_2O_3-doped Bi_2O_3 and La-doped CeO_2 buffer layers

Weimin Guo [a,b,*], Jiang Liu [a,**], Chao Jin [a]

[a] School of Chemistry and Engineering, South China University of Technology, The Key Laboratory of Enhanced Heat Transfer and Energy Conservation, Ministry of Education, Guangzhou 510640, PR China
[b] Department of Biological and Chemical Engineering, Guangxi University of Technology, Liuzhou 545006, PR China

ARTICLE INFO

Article history:
Received 22 February 2010
Received in revised form 13 May 2010
Accepted 22 May 2010
Available online 4 June 2010

Keywords:
Solid oxide fuel cells
Y_2O_3-doped Bi_2O_3
Strontium- and magnesium-doped lanthanum gallate
Composite electrolyte film

ABSTRACT

Anode-supported solid oxide fuel cells (SOFCs) with strontium- and magnesium-doped lanthanum gallate (LSGM) have been developed. A novel buffer layer, yttria-doped bismuth oxide (YDB), has been introduced between the cathode and electrolyte interface, while a conventional buffer layer, lanthanum-doped ceria (LDC), has been used between the anode and electrolyte interface. A cell with a YDB (18 μm)/LSGM (19 μm)/LDC (13 μm) composite electrolyte film showed an open-circuit voltage (OCV) 1.07–1.0 V in the operating temperature range of 500–700 °C. The cell using Ag–YDB composite cathode can achieve 701 mW cm^{-2} maximum power density at 700 °C.

1. Introduction

Strontium- and magnesium-doped lanthanum gallate (LSGM) perovskite-type compounds are considered as promising solid electrolytes for intermediate-temperature solid oxide fuel cell (IT-SOFC) applications. Both the high conductivity of LSGM materials and the expected high performance continue to stimulate research on LSGM thin-film cells [1,2]. Recently, many efforts have been made to fabricate SOFC single cells with LSGM thin electrolyte films [3,4]. However, the preparation of anode-supported LSGM thin films by the co-firing technique appears to be difficult due to the serious reactions between LSGM and the traditionally used anode catalyst Ni at high temperatures. The chemical reactions at high temperatures between the LSGM and NiO can be avoided in an iso-La chemical activity cell [5,6]. A better choice for these IT-SOFCs is to use lanthanum-doped ceria (LDC) as a buffer layer between the LSGM electrolyte and Ni-containing anode. The LDC buffer layer can restrain the reaction of LSGM and NiO, while the LSGM layer can block the electronic conductivity of the LDC electrolyte. There are some previous works [5,7,8] considering LDC/LSGM/LDC tri-layer electrolytes using also a LDC buffer layer to avoid reactivity between cathode and LSGM electrolyte. In these works, the LDC layers were effective in minimizing interdiffusion and reaction [7,8]. On the other hand, the open-circuit voltages (OCVs) of the cells based on LDC/LSGM/LDC trilayer as reported in their previous work were lower than the theoretical electromotive force, which could be due to electronic conductivity in the LSGM layer. Moreover, by increasing the ionic conductivity of the materials used as a buffer layer in the composite electrolyte, it is possible to lower the total electrolyte resistance. Doped Bismuth oxides have an ionic conductivity one order of magnitude higher than that of LDC at comparable temperatures. They are pure oxide conductors and are kinetically stable under oxygen partial pressures above 10^{-13} atm at about 600 °C [9–12]. In the absence of contact with an active reducing agent (such as H_2), doped bismuth oxide, such as erbia-stabilized bismuth oxide (ESB), has been used to block the electron penetration of doped ceria [12,13]. Moreover, due to the higher ionic conductivity of doped bismuth oxide compared to that of doped ceria, higher electrical conductivity of a bilayered doped bismuth oxide and doped ceria composite electrolyte can be expected compared to that of a singly doped ceria electrolyte. Park et al. deposited an ESB film onto samarium-doped ceria (SDC) substrates by a pulsed-laser deposition (PLD) and multicycling dip-coating process. They reported that the effective conductivity of bilayer ESB/samaria-doped ceria (SDC) measured in air in the temperature range from 300 to 800 °C led to higher total conductance values than those of SDC, which confirmed at the very least that no lower

* Corresponding author at: Department of Biological and Chemical Engineering, Guangxi University of Technology, No. 268 Donghuan Road, Liuzhou, Guangxi 545006, PR China. Tel.: +86 772 2687 033; fax: +86 772 2687 033.
** Corresponding author. Tel.: +86 772 2687 033; fax: +86 772 2687 033.
E-mail addresses: guoweimin8@163.com (W. Guo), jiangliu@scut.edu.cn (J. Liu).

0925-8388/$ – see front matter © 2010 Elsevier B.V. All rights reserved.
doi:10.1016/j.jallcom.2010.05.117

conducting phase was formed at the bilayer interface [13]. Chan et al. simulated yttria-doped bismuth oxide (YDB) as the substrate electrolyte and a thin layer of yttria-stabilized zirconia (YSZ) as a coating on the anode side. It was found that depositing a very thin layer of YSZ onto the YDB in a thickness ratio of 1–10,000 (e.g. 10 nm-thick YDB layer and 100 μm-thick YSZ layer) significantly increased the interfacial oxygen partial pressure in the bilayer electrolyte and reduced the penetration of the electronic current [14]. They reported that the fabrication of an ultra thin but dense layer of YSZ onto a substrate electrolyte is technically very difficult and should be overcome. Leng and Chan adopted a cost-effective wet ceramic process/painting/screen-printing method to successfully fabricate a YDB film (of thickness ~16 μm) on gadolinia-doped ceria (GDC) substrates and found that such a YDB film was effective in blocking electronic penetration through the GDC electrolyte [15]. Therefore the investigation of a new YDB/LSGM/LDC trilayer is very interesting, because YDB layer can block the electron penetration of LSGM induced by diffusion of Ni during high temperature co-firing process and it has been reported an increase of the open-circuit voltages using doped bismuth/doped ceria bilayers such as ESB/GDC, YDB/YSZ and YDB/GDC.

As mentioned above, bilayer electrolytes have been commonly introduced to prevent the decomposition of doped bismuth oxide in low partial pressures of oxygen. In order to apply YDB electrolyte to an LSGM electrolyte layer as a buffer layer for IT-SOFCs, we have designed trilayer electrolyte composed of a YDB layer on the oxidizing side and an LSGM/LDC composite layer on the reducing side. The advantage of this design is that LSGM, LDC, and YDB are all sufficiently conductive to serve as IT-SOFC electrolytes. In addition, compared with the previous reports summarized above, YDB is fabricated onto the LSGM electrolyte as a buffer layer, which is also effective in improving the electrochemical performance of the resulting trilayer electrolyte SOFCs [7,8,16,17].

In the present work, a YDB buffer layer has been employed in the fabrication of anode-supported SOFCs with an LSGM electrolyte layer. To the best of our knowledge, there has not hitherto been any report on the application of a YDB/LSGM/LDC composite electrolyte in an anode-supported SOFC in the literature.

2. Experimental

$La_{0.9}Sr_{0.1}Ga_{0.8}Mg_{0.2}O_{3-\delta}$ (LSGM) and $La_{0.4}Ce_{0.6}O_{1.8}$ (LDC) powders were synthesized by conventional solid-state reactions [7]. $Bi_{0.75}Y_{0.25}O_{1.5}$ (YDB) was prepared by reverse-titration chemical co-precipitation from a Bi^{3+}- and Y^{3+}-containing aqueous solution [18]. For this, analytically pure $Bi(NO_3)_3{\cdot}5H_2O$ and $Y(NO_3)_3{\cdot}6H_2O$, in a molar ratio of 3:1, were dissolved in dilute nitric acid to prepare a nitrate solution containing a total metal ion (Bi^{3+}, Y^{3+}) concentration of 0.1 mol L^{-1}. This nitrate solution was added drop wise to aqueous ammonia solution in a reaction vessel at room temperature. The solution was continuously stirred using a magnetic needle and was maintained at around pH 12. During the chemical titration, a 1 wt% solution of PEG4000 (polyethylene glycol of average molecular weight 4000) in aqueous ammonia was added as a dispersing agent. The precipitate was oven-dried at 80 °C and calcined at 750 °C for 2 h to form YDB powder. $Sm_{0.2}Ce_{0.8}O_{1.9}$ (SDC) powder was prepared using a citric–nitrate process and was calcined at 800 °C for 2 h [19]. Nickel oxide (NiO) powder was obtained by the precipitation method, using $Ni(NO_3)_2{\cdot}6H_2O$ as the raw material and ammonia as the precipitant. The precipitate was calcined at 400 °C for 2 h. All of the powders were characterized by X-ray powder diffraction (XRD) on a Shimadzu XD-3A diffractometer with a scanning step of 0.02°.

The as-prepared NiO and SDC powders were mixed in a weight ratio of 6:4. After supplementing the mixture with 15 wt% starch as a pore former, the anode powder was pressed into pellets of diameter 13 mm and thickness 0.6 mm. The green pellets were pre-sintered at 1000 °C for 4 h to obtain the NiO–SDC anode substrates. LSGM/LDC bilayer electrolytes were fabricated by a centrifugal casting technique. In this way, layers of first LDC and then LSGM were sequentially deposited on the NiO–SDC anode substrates [7,20]. The thicknesses of the LSGM and LDC layers were controlled by the amount of slurry. The deposited pellets were co-fired at 1400 °C for 4 h. A YDB layer was also fabricated on the LSGM/LDC by a centrifugal casting technique. The anode substrates with the YDB/LSGM/LDC trilayer were then sintered at 900 °C for 2 h. Before application of the cathodes, the gas tightness of as-fired samples was characterized with a vacuum measurement apparatus as previously described by Dollen and Barnett [21]. The porous cathode was prepared using a mixture of Ag and YDB in a weight ratio of 6:4 with an ethylcellulose–terpineol vehicle [22]. The mixture was applied to the electrolyte and then fired at 600 °C for 2 h in air. The cathode area was 0.20 cm^2.

A single cell was assembled by attaching a cell pellet to one end of an alumina tube using silver paste as a sealant and joint material. The cells were tested with an electrochemical instrument (Autolab PGSTAT30, Holland). Hydrogen was passed over the anode at a flow rate of 75 mL min^{-1}, while the cathode was exposed to ambient air. After reducing the NiO-containing anode at 500 °C in H_2 for several hours, the performance of the cell was tested from 500 to 700 °C. The morphology and microstructure of the single cells were characterized with a Philips XL-30FEG scanning electron microscope (SEM). AC impedance spectroscopy was typically carried out in the frequency range from 0.01 Hz to 100 kHz with a signal amplitude of 20 mV under open-circuit conditions at temperatures between 500 and 700 °C.

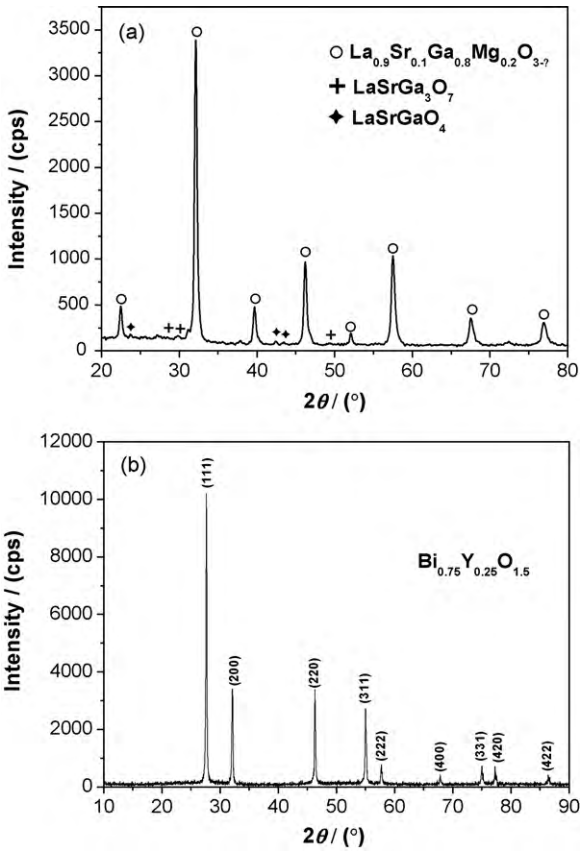

Fig. 1. XRD patterns of the as-prepared powders: (a) LSGM and (b) YDB.

3. Results and discussion

XRD analysis showed the XRD pattern of the as-prepared LSGM powder (Fig. 1a) to be in good agreement with the diffraction data for a perovskite phase, but a few small impurity peaks of $LaSrGaO_4$ and $LaSrGa_3O_7$ can be seen in XRD pattern. The XRD pattern of YDB powder (Fig. 1b) shows good agreement with the expected peaks for a δ-Bi_2O_3 phase, with no indication of any second phase.

Fig. 2 shows SEM images of cross-sectional views of anode-supported SOFCs with the YDB/LSGM/LDC composite electrolyte (Fig. 2). The total thickness of the YDB/LSGM/LDC composite electrolyte film was 50 μm (18 μm YDB + 19 μm LSGM + 13 μm LDC). As can be seen from the SEM images, the YDB, LSGM and LDC trilayers were good intimate contact and surrounded electrodes, showing that the materials sintered well together. The LSGM and LDC layers were relatively dense, and the location of YDB layer closed to LSGM layer was tight while the location away from LSGM layer was actually porous. A further increase in the sintering temperature of the YDB layer would have led to a change in its composition due to the evaporation of bismuth [15]. The obtained YDB layer with a porous microstructure still exhibited good compatibility

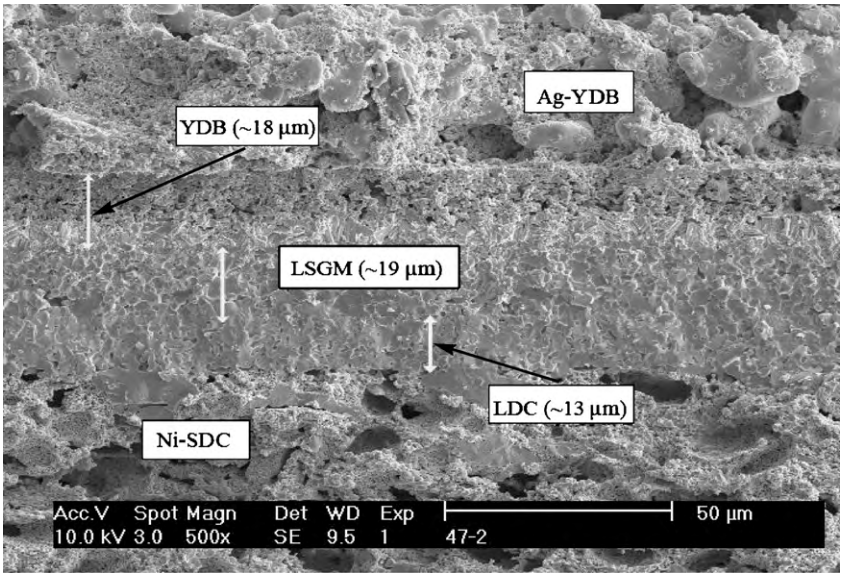

Fig. 2. SEM images of cross-sectional views of the cell with a YBD/LSGM/LDC composite electrolyte.

between the LSGM electrolyte and Ag–YDB cathode, as discussed later, although a dense YDB layer might have been better.

Fig. 3 shows the cell voltages and power densities measured from 500 to 700 °C as a function of current density for the cell. The open-circuit voltage (OCV) of the cell at 700 °C was 1.0 V, indicted that the electron penetration of LSGM induced by diffusion of Ni during high temperature co-firing process was effectively blocked by YDB/LSGM/LDC trilayers. In comparison with our previous work [7], the slight increase of the OCV value may be due to the use of an YDB layer. Correspondingly, the maximum power density was 701 mW cm^{-2} at 700 °C. The cell performance is believed to be due to the effect of its OCV.

Fig. 4 shows the impedance curves of the cell with Ag–YDB cathode measured from 500 to 700 °C under open-circuit conditions. The ohmic resistances and electrode polarization resistances were evaluated from the impedance spectra. The measured specific ohmic resistance was 0.174 Ω cm^2 at 700 °C, observably higher than the calculated value 0.0663 Ω cm^2 of the across the YDB/LSGM/LDC trilayer electrolyte film based on prior reported bulk YDB conductivity of 0.19 S cm^{-1}, LSGM of 0.074 S cm^{-1} and LDC of 0.042 S cm^{-1} at 700 °C [23–25]. This is likely because the bulk conductivity of LDC in a single cell under operating condition is higher than that measured directly on the electrolyte under air atmosphere [26], and the contribution to the ohmic resistance of the electrodes or possible interfacial reactions between the cell components will be convinced in the next study. The polarization resistance of the cell was 0.166 Ω cm^2. That is, the polarization loss was about 50% of the total resistance. Another conclusion from Fig. 4 is that the good cell performance, compared to thin-YSZ electrolyte cells, was due to low polarization resistance rather than low electrolyte resistance. This may be attributed to a low polarization resistance for electrodes in contact with YDB.

In this study, the total thickness of the YDB/LSGM/LDC composite electrolyte was 50 μm, the cathode was Ag–YDB, and the YDB layer was not fully dense (Fig. 2). Leng et al. [15] have reported that the power density may have been significantly improved by using a thinner composite electrolyte with a denser YDB layer and adopting a more active material as the cathode. Furthermore, Ag-containing cathodes such as Ag–$(BaO)_{0.11}(Bi_2O_3)_{0.89}$ [27] or Ag–bismuth oxide [28,29] and Ag–BICUVOX.10 [30] cathodes based on perovskite-based materials such as $La_{0.7}Sr_{0.3}CoO_{3-\delta}$ cathode [31], and bismuth-ruthenate-based cathodes such as $Bi_2Ru_2O_7$

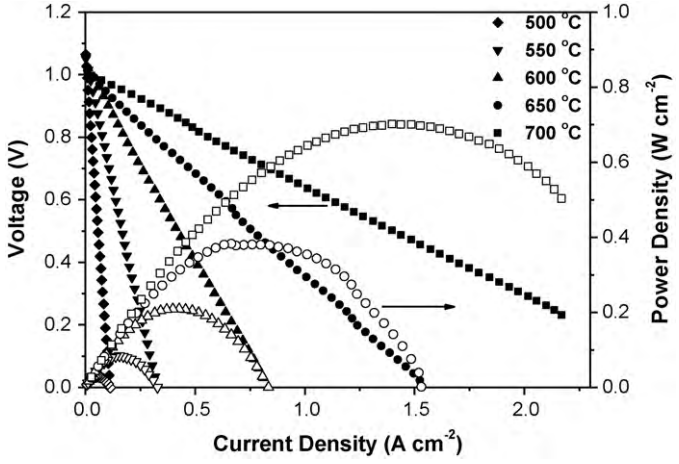

Fig. 3. Voltage and power density as a function of current density of a cell consisting of YDB/LSGM/LDC composite electrolytes operated on air and humidified hydrogen (H_2 flow rate: 75 mL min^{-1}).

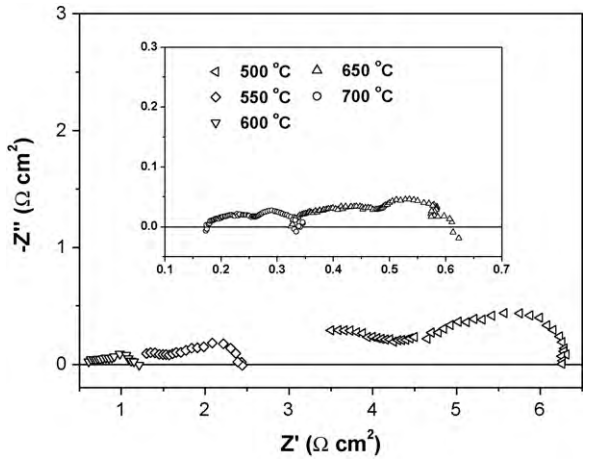

Fig. 4. Electrochemical impedance spectra of a single SOFC consisting of YDB/LSGM/LDC composite electrolytes with an Ag–YDB cathode measured under open-circuit conditions for SOFCs.

[32] may be used in SOFCs with the YDB/LSGM/LDC composite electrolyte.

4. Conclusions

A YDB buffer layer has been deposited on an LSGM/LDC composite electrolyte using a centrifugal casting technique. In this way, anode-supported SOFCs with a trilayered YDB/LSGM/LDC composite electrolyte film have been developed. A cell consisting of a YDB/LSGM/LDC composite electrolyte film using Ag–YDB composite cathode showed that YDB layer can block the electron penetration of LSGM induced by diffusion of Ni during high temperature co-firing process. As a result, the introduction of YDB to an anode-supported SOFC with a LSGM/LDC composite electrolyte film will help the cell to achieve higher power output. These results show the potential application of the YDB/LSGM/LDC composite as a promising electrolyte for IT-SOFCs.

Acknowledgements

The authors gratefully acknowledge financial support from the 863 Program of the National High Technology Research Development Project of China (No. 2007AA05Z136), the Department of Science and Technology of Guangdong Province (No. 2005B50101007) and the Department of Education of Guangdong Province (No. B15N9060210). We also appreciate the financial support from the Key Project of Ministry of Education of China (No. 210163), the Natural Science Foundation of Guangxi Zhuang Autonomous Region (No. 2010GXNSFA013045), the Department of Education of Guangxi Autonomous Region (No. 200911MS113) and Guangxi University of Technology (No. 09304).

References

[1] T. Ishihara, H. Matsuda, Y. Takita, J. Am. Chem. Soc. 116 (1994) 3801–3803.
[2] J.H. Wan, J.Q. Yan, J.B. Goodenough, J. Electrochem. Soc. 152 (2005) A1511–A1515.
[3] J.W. Yan, Z.G. Lu, Y. Jiang, Y.L. Dong, C.Y. Yu, W.Z. Li, J. Electrochem. Soc. 149 (2002) A1132–A1135.
[4] Z.H. Bi, B.L. Yi, Z.W. Wang, Y.L. Dong, H.J. Wu, Y.C. She, M.J. Cheng, Electrochem. Solid-State Lett. 7 (2004) A105–A107.
[5] K.Q. Huang, J.H. Wan, J.B. Goodenough, J. Electrochem. Soc. 148 (2001) A788–A794.
[6] Y. Matsuzaki, I. Yasuda, Solid State Ionics 152–153 (2002) 463–468.
[7] W.M. Guo, J. Liu, Y.H. Zhang, Electrochim. Acta 53 (2008) 4420–4427.
[8] Y.B. Lin, S.A. Barnett, Electrochem. Solid-State Lett. 9 (2006) A285–A288.
[9] N.M. Sammes, G.A. Tompsett, H. Näfe, F. Aldinger, J. Eur. Ceram. Soc. 19 (1999) 1801–1826.
[10] P. Shuk, H.D. Wiemhöfer, U. Guth, W. Göpel, M. Greenblatt, Solid State Ionics 89 (1996) 179–196.
[11] K.Z. Fung, H.D. Baek, A.V. Virkar, Solid State Ionics 52 (1992) 99–104.
[12] E.D. Wachsman, P. Jayaweera, N. Jiang, D.M. Lowe, B.G. Pound, J. Electrochem. Soc. 144 (1997) 233–236.
[13] J.Y. Park, H. Yoon, E.D. Wachsman, J. Am. Ceram. Soc. 88 (2005) 2402–2408.
[14] S.H. Chan, X.J. Chen, K.A. Khor, Solid State Ionics 158 (2003) 29–43.
[15] Y.J. Leng, S.H. Chan, Electrochem. Solid-State Lett. 9 (2006) A56–A59.
[16] T. Ishihara, T. Shibayama, M. Honda, H. Nishiguchi, Y. Takita, Chem. Commun. (1999) 1227–1228.
[17] T. Ishihara, T. Shibayama, H. Nishiguchi, Y. Takita, J. Mater. Sci. 36 (2001) 1125–1131.
[18] Q. Zhen, G.M. Kale, G. Shi, R. Li, W.M. He, J.Q. Liu, Solid State Ionics 176 (2005) 2727–2733.
[19] D.H.A. Blank, H. Kruidhof, J. Flokstra, J. Phys. D: Appl. Phys. 21 (1988) 226–227.
[20] J. Liu, S.A. Barnett, J. Am. Ceram. Soc. 85 (2002) 3096–3098.
[21] P.V. Dollen, S.A. Barnett, J. Am. Ceram. Soc. 88 (2005) 3361–3368.
[22] C.R. Xia, Zhang, M.L. Liu, Appl. Phys. Lett. 82 (2003) 901–903.
[23] D. Singman, J. Electrochem. Soc. 113 (1966) 502–504.
[24] C.B. Choudhary, H.S. Maiti, E.C. Subbarao, Solid Electrolytes and Their Applications, first ed., Plenum Press, New York, 1980, p. 40.
[25] T. Shimonosono, Y. Hirata, S. Sameshima, J. Am. Ceram. Soc. 88 (2005) 2114–2120.
[26] Z.H. Bi, Y.L. Dong, M.J. Cheng, B.L. Yi, J. Power Sources 161 (2006) 34–39.
[27] S.G. Huang, Z. Zong, C.Q. Peng, J. Power Sources 173 (2007) 415–419.
[28] M. Camaratta, E. Wachsman, Solid State Ionics 178 (2007) 1242–1247.
[29] M. Camaratta, E. Wachsman, Solid State Ionics 178 (2007) 1411–1418.
[30] C.R. Xia, M.L. Liu, Adv. Mater. 14 (2002) 521–523.
[31] V.V. Kharton, E.N. Naumovich, V.Y. Samokhval, Solid State Ionics 99 (1997) 269–280.
[32] A. Jaiswal, E.D. Wachsman, J. Electrochem. Soc. 152 (2005) A787–A790.